



Contingency Analysis in the Southern Ethiopian Power Transmission Network using Particle Swarm Optimized Unified Power Flow Controller

Frezer Fikade Asfaw*, Muluneh Lemma Woldesemayat, Samuel Kefale Melese

Faculty of Electrical and Computer Engineering, Arba Minch University, Arba Minch, Ethiopia

*Corresponding Author's Email: adefikade43@gmail.com

Abstract

Frequent line contingencies are a major driver of voltage limit violations and transmission line overloads within the southern power network, which comprises 28 lines and 27 buses. This paper analyzes the effects of single-line contingencies and proposes using a Unified Power Flow Controller (UPFC) to mitigate voltage violations and line overloading. A MATLAB tool was used to simulate the network under single line outage scenarios, both before and after the integration of the UPFC. The optimal placement and parameter settings of the UPFC are determined using a performance index and the Particle Swarm Optimization (PSO) technique. The results indicate that the outages of lines 1, 20, 6, 17, and 19 are the most critical, in descending order. In particular, the outage of line 1 resulted in 23 overloaded lines and 21 buses operating beyond their voltage limits. However, by installing a 75 MVAR UPFC at line 6, the violations were significantly reduced to one overloaded line and no buses outside the normal voltage range. The results demonstrate that optimally placed UPFC significantly enhances voltage stability and transmission capacity under N-1 contingencies.

Keywords: MATLAB, Particle swarm optimization, Performance index, Single line contingency, Southern Ethiopia, Transmission line overloading, Unified power flow controller

I. INTRODUCTION

To supply reliable and secure electricity to end-users, proper coordination among power system elements is essential. However, the sudden loss or failure of any one of these elements can disturb the operation of the remaining components and affect the customers. This phenomenon is referred to as contingency. Contingencies are the primary causes of transmission line overloading and voltage limit violations at buses, which may finally lead to successive outages and, in severe cases, partial or total blackouts [1, 2].

Therefore, contingency analysis is necessary in modern power systems to evaluate the network's

Received: May 23, 2026; Revised: June 1, 2026; Accepted: June 19, 2026; Published: June 25, 2026

Corresponding author- Frezer Fikade Asfaw



behavior before such events occur. It serves as a "what-if" assessment to examine power system security under the outage of major components such as generators, transmission lines, and transformers [3]. Historically, most blackouts have resulted from the successive failure of power system elements due to overloaded lines [4]. According to data from the Ethiopian National Load Dispatch Center, approximately 82 lines' outages were recorded in the southern region between November 1, 2020, and April 30, 2021. Notably, the outage of the Gibe III to W/Sodo II transmission line caused three nationwide blackouts within six months. Several other line outages also led to partial blackouts.

The main causes of these outages included earth faults, overcurrent, undervoltage, underfrequency, and protection failures. For instance, on April 13, 2021, the outage of the Gibe III to W/Sodo II line was caused by a busbar differential protection trip at the W/Sodo II substation, resulting in a blackout that lasted approximately 50 minutes. Given these risks, contingency analysis is a critical task for power system planners and operators. It helps predict the extent of violations that may occur during unexpected outages and enables timely preventive or corrective actions [5, 6]. Continuous evaluation of network contingencies is one of the most effective strategies for minimizing or eliminating outages in power systems [7].

Contingency, as defined by the North American Electric Reliability Council (NERC), is an unanticipated outage of a system component such as a generator, transmission line, or circuit breaker that can cause significant changes in the system's operation and design [8 -10]. Contingency analysis involves simulating each possible single outage and typically includes the following three steps [11]: -

i. **Contingency creation**

The first stage of contingency analysis involves contingency creation, which is the process of listing all probable network outage scenarios. In this study, 28 contingencies were considered, corresponding to the 28 transmission lines in the system.

ii. **Contingency screening or ranking**

This stage is performed to select or screen the most severe outage that leads to the overloading of transmission lines and bus voltage limit violations. Then, the severe lines are ranked in descending order in terms of their severity using performance index methods.



iii. Contingency evaluation

This is the last stage, the critical outage is identified and ranked, and the preventive and corrective actions are performed using different methods. In this study, the UPFC is chosen to remove or eliminate the overloaded transmission line and voltage limit-violating buses.

II. MATERIALS AND METHODS

Method of Contingency Analysis

Contingency analysis is time-consuming, as it requires computing the effects of every possible outage scenario. The N-1 contingency is considered in this study. To address this, an automatic contingency screening approach is employed. This identifies and ranks only those outages that significantly affect the power flow in transmission lines or cause voltage deviations at buses.

Several methods can be used to analyze the most critical contingencies. One such approach involves sensitivity factor methods, which are categorized into Generator Shift Factors (GSF) and Line Outage Distribution Factors (LODF). The DC load flow method used in these techniques is non-iterative, fast, and effective for estimating active power flow in transmission lines. It cannot evaluate the reactive power flow or assess the voltage profile of the network [5, 12, 13]. Therefore, sensitivity factor methods that rely on DC load flow are not suitable for this study.

Another approach is the Performance Index (PI) method, which is further classified into the Voltage Performance Index (VPI) and Active Power Performance Index (PIP). In this study, the PI method is adopted for contingency analysis because it utilizes the AC load flow method, which can evaluate both power flow and voltage profiles. The two types of performance indexes, active power and voltage, are defined below [14, 15].

$$P_{ip} = \sum_{i=1}^L \left(\frac{w}{2n}\right) \left(\frac{S_i}{S_{max}}\right)^{2n} \quad (1)$$

Where, P_{ip} is the performance index for active power, L = Total number of the transmission lines, w = real non-negative weighting factor (1), n = a penalty function (1), S_i = Apparent power flow in line i from load flow and $S_{i max}$ = is the maximum carrying capacity of the line i . P_{iv} represents the violation of bus voltage magnitude and is mathematically given as follows:

$$P_{iv} = \sum_{i=1}^{n-m-1} \left(\frac{w}{2n}\right) \left(\frac{(V_i - V_{i nom})}{(V_{i max} - V_{i min})}\right)^{2n} \quad (2)$$



Where, n = Overall number of buses existing in the network, m = Total number of PV buses existing in the system, $m-1$ = The total number of load buses existing in the network, V_i = Voltage of bus i after load flow, $V_i \text{ nom}$ = Nominal voltage at bus i , $V_i \text{ min}$ = Minimum voltage limit and assumed as 90% of $V_i \text{ nom}$ and $V_i \text{ max}$ = Maximum voltage limit and assumed as 110% of $V_i \text{ nom}$.

UPFC Power Injection Model

The UPFC was invented for the real-time control action and dynamic compensation of an AC system. Maintaining the multifunctional flexibility is needed to mitigate the process of power delivery problem. It can control all the line parameters which can harm the power flow (i.e., voltage magnitude, phase angle, and line impedance) independently and simultaneously [16, 17].

UPFC also has the unique ability to control real and reactive power flow on a transmission line system, as well as to regulate the voltage at the buses where it is connected. At the same time, it can increase the security of the system by increasing the limit of transient stability, reducing the value of the reactive power. It will also optimize the flow of real power through the transmission lines [18].

The UPFC can be represented by one voltage source $V_{se} < \delta_{se}$, one current source converter (I_{sh}) and the impedance being the leakage of the reactance of the coupling transformer. The series-connected voltage source converter is controllable in both magnitude and phase angle, whereas the shunt current source converter is controllable only in magnitude. The steady-state equivalent circuit is given in Fig. 1.

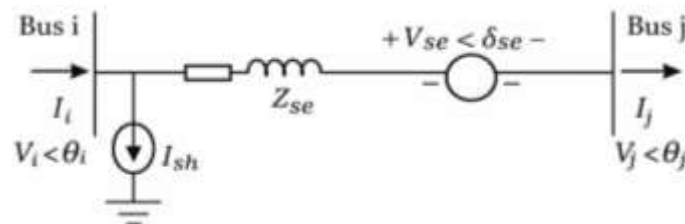


Fig.1. Equivalent circuit representation of UPFC

From the equivalent circuit of UPFC given in Fig. 1, the power injection model is given in Fig. 2.

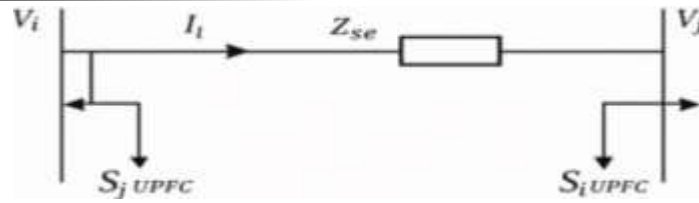


Fig. 1. Power injection model of UPFC

The mathematical model of power injected into the lines is given by the following equation:

$$S_i^{UPFC} = V_i \left(\frac{V_{se}}{Z_{se}} \right)^* - V_i (I_{sh})^* \quad (3)$$

$$S_j^{UPFC} = V_j \left(\frac{V_{se}}{Z_{se}} \right)^* \quad (4)$$

Where, V_i is the sending end and V_j is the receiving end voltage, which can be represented as $V_i = |V_i| \angle \theta_i$ and $V_j = |V_j| \angle \theta_j$, respectively. V_{se} is the series-connected voltage source converter of UPFC and given by $V_{se} = |V_{se}| \angle \delta_{se}$, I_q is the shunt injected reactive current of UPFC, Z_{se} is the series impedance of coupling transformer, respectively.

Then, the injected real and reactive power equation of the UPFC linked to the transmission line between the sending end i and receiving end bus j is given by:

$$P_i^{UPFC} = -G_{se} V_{se}^2 + 2G_{se} V_i V_{se} \cos(\theta_i - \delta_{se}) - V_j V_{se} (G_{se} \cos(\theta_i - \delta_{se}) - B_{se} \sin(\theta_i - \delta_{se})) \quad (5)$$

$$Q_i^{UPFC} = V_i V_{se} (G_{se} \sin(\theta_i - \delta_{se}) - B_{se} \cos(\theta_i - \delta_{se})) - V_i I_q \quad (6)$$

$$P_j^{UPFC} = -V_j V_{se} (G_{se} \cos(\theta_j - \delta_{se}) + B_{se} \sin(\theta_j - \delta_{se})) \quad (7)$$

$$Q_j^{UPFC} = -V_j V_{se} (G_{se} \sin(\theta_j - \delta_{se}) - B_{se} \cos(\theta_j - \delta_{se})) \quad (8)$$

Particle Swarm Optimization

The PSO is a powerful evolutionary algorithm that is based on the social behavior of bird flocking and fish schooling, and it is a population-based stochastic search approach. A study originally proposed the concept of PSO in 1995 [19, 20]. It is simple to construct, computationally inexpensive, and requires little memory and CPU performance. The algorithm iteratively updates the series injected voltage magnitude, phase angle, and shunt reactive current to minimize an objective function stated as a contingency performance index, while satisfying power system



operating constraints. It also requires no information about the objective function, such as the gradient, but only the value [7].

The velocity and position of each particle are updated using the expression below [21]:

$$V_i^{k+1} = WV_i^k + C1 * R1(Pbest_i - X_i^k) + C2 * R2(gbest_i - X_i^k) \quad (9)$$

$$X_i^{k+1} = X_i^k + V_i^{k+1} \quad (10)$$

Where C1 and C2 are cognitive and social acceleration constants, respectively, k is the iteration count, i is the particle number, V is velocity, X is position, R1 and R2 are two random numbers, pbest is personal best position, gbest is global best position, and finally w is the inertia weight factors and given by the formula given below:

$$W = W_{max} - (W_{max} - W_{min}) * iter/itmax \quad (11)$$

Where W_{max} and W_{min} are the initial and final inertia weight, respectively, iter is iteration number and itmax is maximum iteration number.

Objective Function for Single Line Outage

The main objective of this study is to eliminate or reduce the line overloading and voltage limit violations due to the outage of a single line from the proposed network using PSO based unified power flow controller.

$$\text{Objective function: Min } \sum_{l=1}^{nl} \left(\frac{S_l}{S_{max}} \right)^2 + \sum_{i=1}^{nb} \left(\frac{V_i - V_{i,ref}}{V_{i,ref}} \right)^2 \quad (12)$$

Where, nl = Total number of transmission lines, nb is the number of buses, S_i = Apparent power flow in line i , S_i max = is the maximum carrying capacity of the line i , V_i is the bus voltage magnitude at bus i , and $V_{i,ref}$ is the reference bus voltage magnitude at bus i . The equality and inequality constraints optimization problems are given as follows:

i Equality constraints

The power flow equation represents the equality constraints of each particle which are performed by running the Newton-Raphson load flow algorithm and given as follows:

$$P_{gi} - P_{di} - V_i \sum V_j (G_{ij} \cos \theta_{ij} + B_{ij} \sin \theta_{ij}) = 0 \quad (13)$$

$$Q_{di} - V_i \sum V_j (G_{ij} \sin \theta_{ij} - B_{ij} \cos \theta_{ij}) = 0 \quad (14)$$



ii Inequality constraints

The inequality constraints are the system operating constraints and are grouped into control variables and state variables. The control variables are the UPFC parameters. The state includes reactive power generation, load bus voltage, and line flow limit. The variables are restricted by adding a quadratic penalty term to the objective function and the constraints are given as follows:

- 1) The voltage magnitude limit at each bus

$$V_i^{min} < V_i < V_i^{max} \quad (15)$$

- 2) The reactive power generation limit Q_{gi} for each generator bus

$$Q_{gi}^{min} < Q_{gi} < Q_{gi}^{max} \quad (16)$$

- 3) The thermal limit for each transmission line

$$S_l < S_l^{max} \quad (17)$$

- 4) The UPFC variables constraints are;

Series injected voltage, $0.0001 < V_{se} < 0.2$ p.u, Phase angle of the series injected voltage, $0 < \delta_{se} < 2\pi$ rad and Shunt connected current, $-0.15 < I_q < 0.15$ p.u.

III. ANALYSIS AND RESULTS

A. Modelling of the Proposed Network

The Ethiopian Electric Power (EEP) is the unique provider of electricity to the nation and neighboring countries such as Sudan and Djibouti. Based on Geographical location, EEP is classified into nine regions namely: Addis Ababa, Central, Eastern, Northeastern, Northern, Northwestern, Southern, Southwestern, and Western regions [22]. Among the nine regions, this work is focused on 132kV, 230kV, and 400kV transmission lines of the Southern regions. As the name indicates, it is located in the southern part of the country, and it consists of 2 generators, 4 external grids, 27 buses, and 28 transmission lines.

A modern power system typically consists of a generator, transformer, transmission line, compensating devices, loads, and other components. Representing all these elements within a single frame is challenging. To address this difficulty, the concept of a one-line diagram is adopted in power system analysis. The one-line diagram of the southern network is shown in Fig. 3.

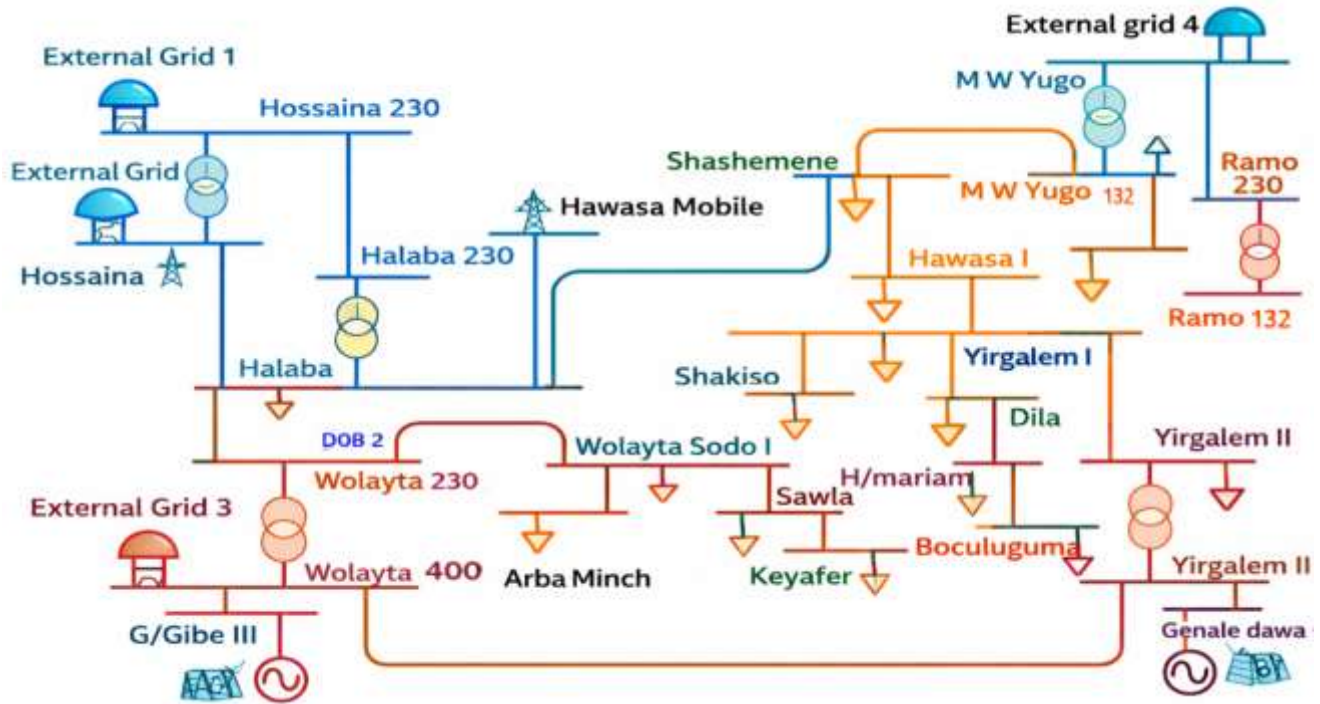


Fig. 3. Single-line diagram of the southern region of the Ethiopian power system

B. Transmission Line and Load Data

This data is collected from the Hawassa District and National Load Dispatch Center archive of the Ethiopian national grid located at Gerji Mebrat Hail, Ethiopia.

TABLE I
LOAD DATA OF THE SOUTHERN NETWORK

Bus number	Bus name	Peak load demand	
		(MW)	(MVAR)
3	Wolayta 230	4.1342	2.0011
6	Alaba	6.6148	3.0216
7	Hossaina	17.2385	9.2969
8	Hawassa mobile	11.4694	5.5491
11	Wolayta Sodo I	9.8438	4.0172
12	Arba Minch	15.6316	7.5698
13	Sawla	2.3772	3.6175
14	Keyafer	1.5917	0.7704

Received: May 23, 2026; Revised: June 1, 2026; Accepted: June 19, 2026; Published: June 25, 2026

Corresponding author- Frezer Fikade Asfaw



15	Shashemene	20.8476	8.7520
16	Hawassa I	28.6709	12.4134
17	Yirgalem I	7.6485	2.0341
18	Yirgalem II	11.4279	5.5329
19	Shakiso	8.1216	3.2694
20	Dila	8.4754	3.9077
21	Hagere Mariam	6.5781	3.1925
22	Boculuguma	2.8699	1.3915
23	Melakwakena Yugo	11.4981	3.8020
25	Yadot	0.8785	0.4251
27	Ramo	8.4836	4.1037

TABLE II

THE PER UNIT (P.U) VALUE OF EXISTING SOUTH REGIONS 400/230/132 KV
TRANSMISSION LINE AND TRANSFORMER DATA

NL	From Bus Name	To Bus Name	Voltage (kV)	Line R (Pu)	Line X (Pu)	Charging B (Pu)	Rating (MVA)
1	Gibe III	Wolayta 400	400	0.0010	0.0083	0.0178	1973
2	Wolayta 400	Yirgalem II 400	400	0.0024	0.0197	0.0779	1973
3	Wolayta 400	Wolayta 230	400/132	0.0012	0.0191	0.0000	250
4	Yirgalem II 400	Genale Dawa III	400	0.0057	0.0444	0.0769	1973
5	Yirgalem II 400	Yirgalem II	400/132	0.0029	0.0191	0.0000	250
6	Wolayta 230	Halaba	132	0.0397	0.1500	0.0145	89
7	Wolayta 230	W. Sodo I	132	0.0193	0.0364	0.0035	89
8	Halaba	Halaba 230	230/132	0.0092	0.0823	0.0000	40
9	Halaba	Hawassa mobile	132	0.1032	0.1942	0.0188	82
10	Halaba	Hossaina	132	0.0511	0.0961	0.0093	89
11	Halaba	Shashemene	132	0.0815	0.1535	0.0149	89
12	Halaba 230	Hossaina 230	230	0.0184	0.0243	0.0367	402
13	Hossaina 230	Hossaina	230/132	0.0147	0.0523	0.0000	63
14	W. Sodo I	Arba Minch	132	0.1407	0.2649	0.0257	89
15	W. Sodo I	Sawla	132	0.1517	0.3035	0.0292	91

Received: May 23, 2026; Revised: June 1, 2026; Accepted: June 19, 2026; Published: June 25, 2026

Corresponding author- **Frezer Fikade Asfaw**



16	Sawla	Keyafer	132	0.1442	0.2717	0.0261	115
17	Shashemene	Hawassa I	132	0.0323	0.0526	0.0051	82
18	Shashemene	M-W-Yugo	132	0.1537	0.2893	0.0280	89
19	Hawassa I	Yirgalem I	132	0.0525	0.0855	0.0082	89
20	Yirgalem I	Yirgalem II	132	0.0229	0.0779	0.0094	91
21	Yirgalem I	Shakiso	132	0.0392	0.0244	0.0311	82
22	Yirgalem I	Dila	132	0.0489	0.0579	0.0094	91
23	Dila	Hager Mariam	132	0.0101	0.2203	0.0212	91
24	Hager Mariam	Boculuguma	132	0.0945	0.2549	0.0534	115
25	M-W-Yugo	M-W-Yugo 230	230/132	0.0047	0.0523	0.0000	63
26	M-W-Yugo	Yadot	132	0.0335	0.1848	0.0715	91
27	M-W-Yugo 230	Ramo 230	230	0.0503	0.1449	0.0189	402
28	Ramo 230	Ramo	230/132	0.0058	0.0653	0.0000	50

C. Simulation Result

TABLE III

LOADED LINE AND VIOLATED BUS VOLTAGE DURING THE OUTAGE OF THE SEVERE LINE BEFORE AND AFTER UPFC

Tripped line		Before placing UPFC				UPFC		After placing UPFC				Rank
From bus	To bus	Line No.	% loading	Line Bus No.	Voltage magnitude	Placement	Parameter	Line No.	% loading	Line Bus No.	Voltage magnitude	



Gibe III (bus 1) Wolayta 400 (bus 2)	2	272.0700	Bus 3	-0.0587	6	$V_{se} = 0.0345$ $\delta_{se} = 0.4190$ $I_q = 0.1175$	7	483.0595	-	-	1			
	3	664.4900	Bus 5	-0.8725			-	-	-	-	-			
	4	123.5200	Bus 6	0.6962			-	-	-	-	-			
	5	449.6100	Bus 7	0.0030			-	-	-	-	-			
	6	904.9400	Bus 8	-0.0106			-	-	-	-	-			
	7	738.9400	Bus 11	-0.5618			-	-	-	-	-			
	8	1,458.2200	Bus 12	0.0507			-	-	-	-	-			
	9	256.9100	Bus 13	-0.0175			-	-	-	-	-			
	10	628.9500	Bus 14	0.0097			-	-	-	-	-			
	11	340.7600	Bus 15	0.2298			-	-	-	-	-			
	12	996.0200	Bus 16	-0.3171			-	-	-	-	-			
	13	6,320.0800	Bus 17	0.3951			-	-	-	-	-			
	15	108.1500	Bus 18	-0.4466			-	-	-	-	-			
	17	186.0000	Bus 19	-5.2644			-	-	-	-	-			
	19	182.530000	Bus 20	0.6003			-	-	-	-	-			
	20	361.4400	Bus 21	-0.3915			-	-	-	-	-			
	21	35,127.200	Bus 22	-0.0700			-	-	-	-	-			
	22	558.4100	Bus 23	-0.2670			-	-	-	-	-			
	23	1584.4500	Bus 25	-0.0017			-	-	-	-	-			
	24	169.2600	Bus 26	0.3724			-	-	-	-	-			
	25	3971.5500	Bus 27	-0.1596			-	-	-	-	-			
	27	211.6000	-	-			-	-	-	-	-			
	28	425.5700	-	-			-	-	-	-	-			
	Yigralem I (17) Yirgalem II (18)	6	227.7934	Bus 15			0.8519	11	$V_{se} = 0.1955$ $\delta_{se} = 5.4889$ $I_q = 0.0695$	-	-	-	-	2
		8	140.2387	Bus 16			0.8087			-	-	-	-	-
		11	147.3655	Bus 17			0.7708			-	-	-	-	-
		25	108.1670	Bus 19			0.7641			-	-	-	-	-
				Bus 20			0.7521			-	-	-	-	-
			Bus 21	0.7487	-	-	-			-	-			
		Bus 22	0.7471	-	-	-	-	-						
Wolayta 230 (5) Halaba (6)	17	144.7265	-	-	18	$V_{se} = 0.1765$ $\delta_{se} = 4.8184$ $I_q = 0.0513$	17	136.5801	-	-	3			
	19	169.5000	-	-			20	164.3864	-	-	-			
	20	200.0638	-	-			-	-	-	-	-			
Shashemene (15) Hawassa I (16)	6	103.9735	-	-	6	$V_{se} = 0.1319$ $\delta_{se} = 1.3090$ $I_q = -0.0197$	-	-	-	-	4			

Received: May 23, 2026; Revised: June 1, 2026; Accepted: June 19, 2026; Published: June 25, 2026

Corresponding author- Frezer Fikade Asfaw



Hawassa I (16)	Yirgalem I (17)	6	149.9624	-	-	6	$V_{se} = -0.1884$ $\delta_{se} = 1.0281$ $I_q = -0.0885$	-	-	-	-	5
----------------	-----------------	---	----------	---	---	---	---	---	---	---	---	---

Tables I and II present the load data and per-unit value in the Southern Network. Table III presents the deviated buses from the nominal voltage limits and the overloaded lines before and after the installation of the UPFC. The most critical lines were evaluated and ranked using the voltage performance index (PIv) and the power performance index (PIp). The ranking process is performed for all branch outages individually, considering voltage violations outside the range of 0.9 to 1.1p.u. and line loading violations exceeding the rated power carrying capacity (i.e., 100% loading). The most severe line outages are then arranged in descending order based on PIv and PIp values. An outage with a performance index of zero is considered the least severe contingency, indicating that it does not affect system operation.

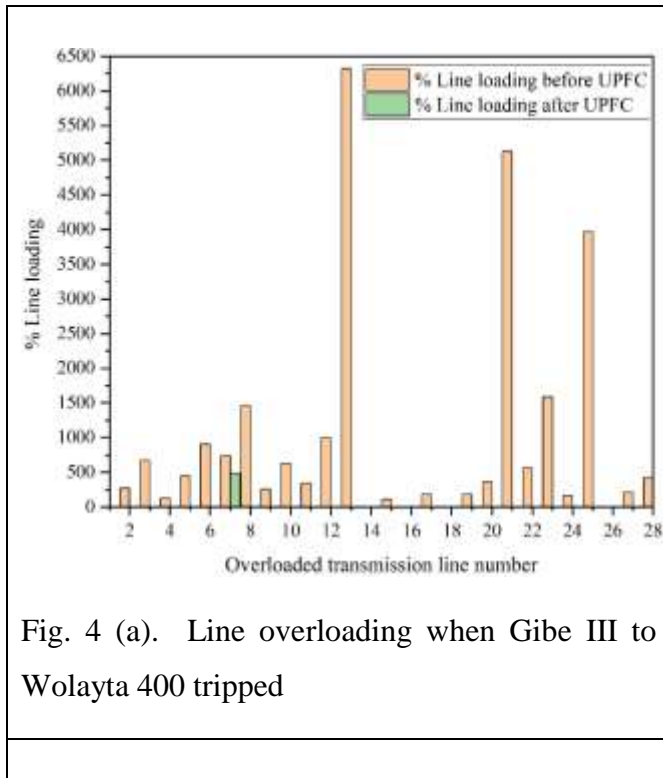


Fig. 4 (a). Line overloading when Gibe III to Wolayta 400 tripped

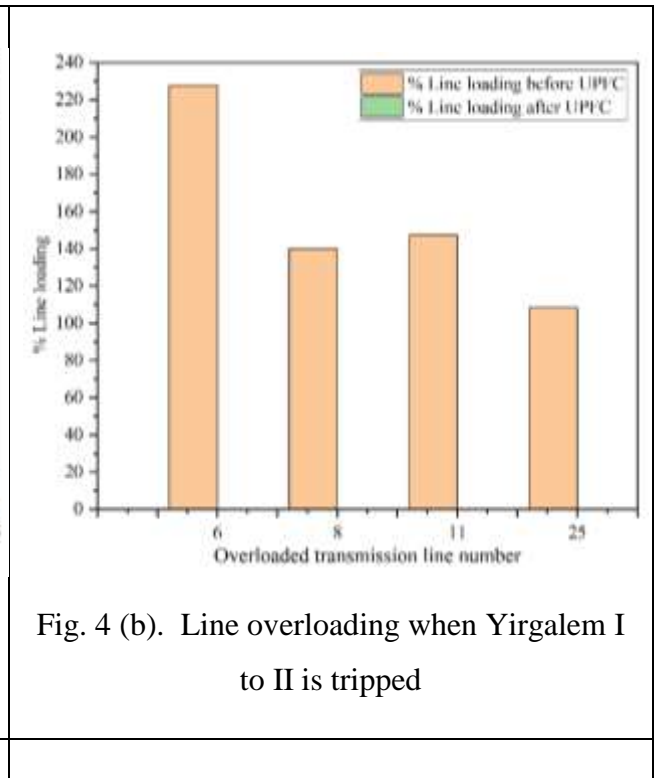


Fig. 4 (b). Line overloading when Yirgalem I to II is tripped

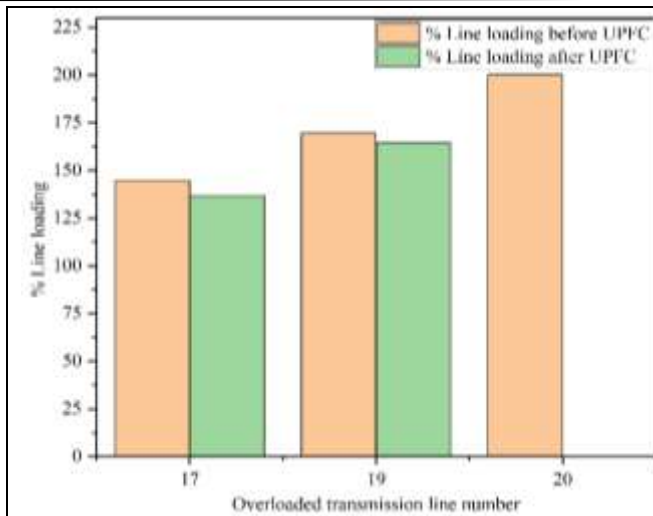


Fig.4 (c). Line overloading when Wolayta II to Halaba is tripped

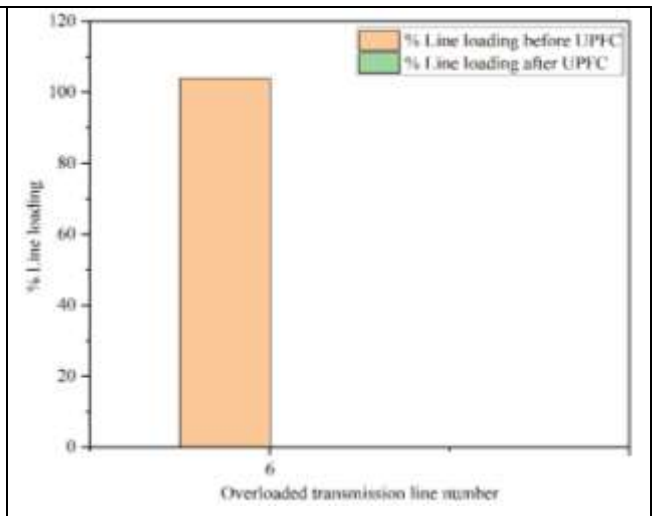


Fig. 4 (d). Line overloading when the Shashemene to Hawassa I is tripped

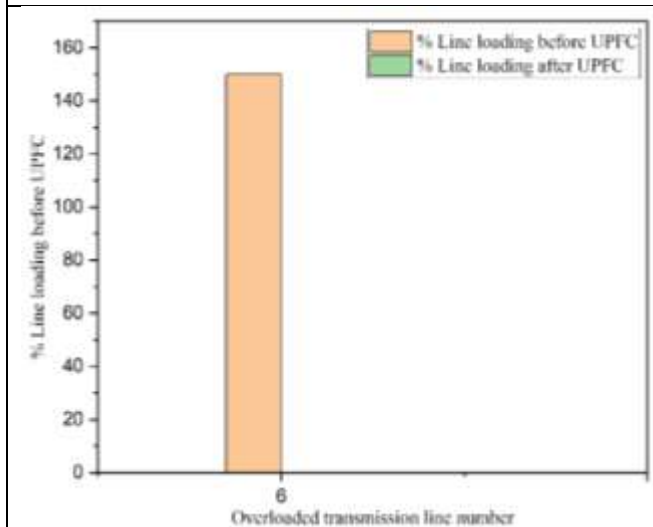


Fig. 4 (e). Line overloading when Hawassa I to Yirgalem I tripped

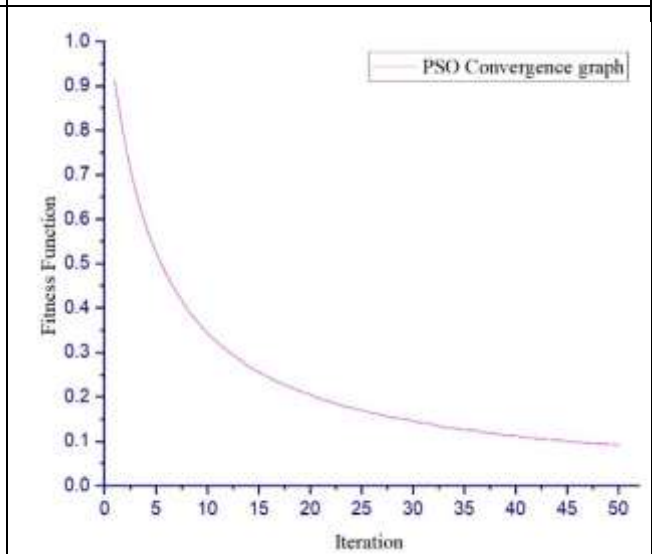


Fig. 4 (f). PSO Convergence graph

Fig. 4 (a) to 4 (f) provide a graphical representation of the overloaded lines listed in Table III. The bar graphs compare the number of overloaded lines with and without UPFC during outages of the most critical lines. Fig. 4 (a) shows that during the outage of Line 1, the number of overloaded lines decreases from 23 to 1 with UPFC. In Fig. 4 (b), the outage of Line 20 shows a reduction from 2 to 0. Fig. 4 (c) shows that during the outage of Line 6, the number decreases from 3 to 2. Fig. 4 (d) indicates that the outage of Line 17 reduces the number from 1 to 0, and Fig. 4 (e) shows

Received: May 23, 2026; Revised: June 1, 2026; Accepted: June 19, 2026; Published: June 25, 2026

Corresponding author- **Frezer Fikade Asfaw**



the same reduction (1 to 0) for the outage of Line 19. These results clearly demonstrate that UPFC can restore overloaded lines to their normal operating state.

The convergence plot in Fig. 4 (f) illustrates a steady decrement in fitness function value over the course of 50 iterations. Initially, the fitness function value was close to 0.95, indicating that power loss, voltage limit deviations, and line overloading were high. Gradually, a remarkable improvement occurred between the 10th and 15th iterations, where the fitness function value decreased significantly. As the process approached the maximum limit of 50 iterations, the value neared 0.09, indicating that convergence tended toward the optimal solution.

TABLE IV

THE TOTAL NUMBER OF VIOLATED BUSES AND OVERLOADED TRANSMISSION LINES WITH AND WITHOUT UPFC

Tripped line			Before UPFC placement			After UPFC placement					
Line Number	From Bus	To Bus	Number of Overloaded Lines	Number of Voltage Violation Bus (NVVB)	Total PI = (NOLL+NVVB)	Number of Overloaded Lines (NOLL)	Number of Voltage Violation Bus (NVVB)	Total PI = (NOLL+NVVB)	Number of Improved Lines	Number of Improved Buses	Rank
1	1	2	23	21	44	1	0	1	22	21	1
4	3	4	-	-	-	unsolved	-	-	-	-	-
20	17	18	2	7	9	0	0	0	2	7	2
6	5	6	3	0	3	2	0	2	1	0	3
17	15	16	1	0	1	0	0	0	1	0	4
19	16	17	1	0	1	0	0	0	1	0	5

Table IV shows the compact form of the most critical outages in terms of the total number of violations for each line outage. According to this result, the outage of line 1 is ranked 1st with 23 overloaded lines and 21 violated buses. In the same manner lines 20, 6, 17, and 19 are ranked as 2nd, 3rd, 4th, and 5th, respectively, with 1 unsolved line (line 4).



The main purpose of this study is to maintain better voltage profiles and power transfer capability in the proposed network using a UPFC during a single-line outage. Therefore, with proper placements and optimal parameter settings of UPFC in the network as shown in Table IV, most of the bus voltage that deviated from the normal operating range of $\pm 10\%$ were kept within an acceptable range. Similarly, the overloaded lines are brought to the normal power carrying capacity.

IV. CONCLUSION

The increasing demand for electrical energy has heightened the need for reliable and efficient power delivery. However, ensuring a stable and secure electricity supply remains a major challenge in the southern region of the Ethiopian power system. This study focused on minimizing violations of the normal operating limits of power system parameters through the application of a Unified Power Flow Controller (UPFC). To integrate the UPFC into a 27-bus system, a modified Newton-Raphson load flow analysis was carried out under both steady-state and N-1 contingency conditions using MATLAB R2019a. A custom MATLAB program was developed to evaluate the network's performance during single-line outages, both before and after the inclusion of the UPFC. The combined voltage and power performance index results revealed that the outages of lines 1, 20, 6, 17, and 19 were the most critical. However, their impact was significantly mitigated by the application of a UPFC. For example, during the outage of Line 1, the number of bus voltage violations decreased from 21 to 0, and the number of overloaded lines dropped from 23 to 1 by optimally placing a 75 MVAR UPFC at Line 6. Similar improvements were observed for other critical outages. This study demonstrated the effectiveness of an optimally placed and rated UPFC in enhancing power system operation by maintaining voltage profiles and transmission line loadings within acceptable limits, thereby supporting the reliable delivery of electric power to end users.

Acknowledgments

The author would like to thank the Ethiopian Electric Power (EEP) for providing real data.

Declaration of Competing Interest

The authors declare no known conflict of interest in this article.

Funding: The authors received no funding for this study.



REFERENCES

- [1] C. D. Iweh, S. Gyamfi, E. Effah-Donyina, and E. Tanyi, “Analysis of contingency scenarios towards a suitable transmission pathway in the southern interconnected grid (SIG) of Cameroon,” *e-Prime - Advances in Electrical Engineering, Electronics and Energy*, vol. 7, p. 100486, Mar. 2024.
- [2] M. S. Geremew, Y. G. Workie, and L. B. Techane, “Identification of system exposure for the northwest region of Ethiopian Electric Power,” *Iran. J. Sci. Technol. Trans. Electr. Eng.*, vol. 48, no. 2, pp. 877–887, Apr. 2024.
- [3] N. S. Swaroop and M. Lekshmi, “Contingency analysis and ranking on 400 kV Karnataka network by using MiPower,” *Int. Res. J. Eng. Technol.*, vol. 3, no. 10, pp. 248–251, Oct. 2016.
- [4] H. Haes Alhelou, M. E. Hamedani-Golshan, T. C. Njenda, and P. Siano, “A survey on power system blackout and cascading events: Research motivations and challenges,” *Energies*, vol. 12, no. 4, p. 682, Feb. 2019, doi: 10.3390/en12040682.
- [5] Y. Salami, “Multiple contingency analysis of power systems,” M.Eng. thesis, Dept. Electr. Comput. Eng., Memorial Univ. Newfoundland, St. John's, NL, Canada, Oct. 2017.
- [6] H. Mirshekali, A. Q. Santos, and H. R. Shaker, “A survey of time-series prediction for digitally enabled maintenance of electrical grids,” *Energies*, vol. 16, no. 17, p. 6332, Aug. 2023.
- [7] I. A. Adejumobi, O. O. Ojetola, and O. D. Adekoya, “Evaluation of power system contingency using performance index,” *ABUAD J. Eng. Res. Dev.*, vol. 1, no. 1, pp. 105–114, Oct. 2017.
- [8] *Glossary of Terms Used in NERC Reliability Standards*, North American Electric Reliability Corporation (NERC), Atlanta, GA, USA, 2026. [Online]. Available: <https://www.nerc.com>. Accessed: Jun. 20, 2026.
- [9] Y. Jiang *et al.*, “Contingency probability estimation for risk-based planning studies using NERC's outage data and standard TPL-001-4,” in *Proc. North Amer. Power Symp. (NAPS)*, Nov. 2021, pp. 1–6.



- [10] Y. Li, Y. Li, and Y. Sun, "Online static security assessment of power systems based on LASSO algorithm," *Appl. Sci.*, vol. 8, no. 9, p. 1442, Aug. 2018.
- [11] T. L. Kumissa and F. Shewarega, "Transient Stability-Based Fast Power System Contingency Screening and Ranking," *Electricity*, vol. 5, no. 4, pp. 947–971, Nov. 2024, doi: 10.3390/electricity5040048.
- [12] H. Zhou, K. Yuan, C. Lei, and J. Guo, "Security Constrained Unit Commitment Based on Modified Line Outage Distribution Factors," *IEEE Access*, vol. 10, pp. 25258–25266, Mar. 2022, doi: 10.1109/ACCESS.2022.3156081.
- [13] D. L. Alvarez, M. Gaha, J. Prévost, A. Côté, G. Abdul-Nour, and T. J.-M. Meango, "N-k static security assessment for power transmission system planning using machine learning," *Energies*, vol. 17, no. 2, p. 292, 2024, doi: 10.3390/en17020292.
- [14] D. B. Aeggegn, A. O. Salau, and Y. Gebru, "Load flow and contingency analysis for transmission line outage," *Arch. Electr. Eng.*, vol. 69, no. 3, pp. 581–594, Sep. 2020.
- [15] R. Tiwari, S. Shrivastava, A. Gupta, and S. Chatterji, "Contingency analysis of complex power system using active power and voltage performance index," in *Advances in Power System Analysis*, Singapore: Springer, 2021, ch. 33, pp. 387–400, doi: 10.1007/978-981-16-1220-6_33.
- [16] F. Banakhr, "Unified power flow controller control strategies for power flow," *Yanbu J. Eng. Sci.*, vol. 19, no. 2, pp. 62–77, Jun. 2022.
- [17] A. N. Alsammak and H. A. Mohammed, "A literature review on the Unified Power Flow Controller (UPFC)," *Int. J. Comput. Appl.*, vol. 182, no. 12, pp. 23–29, Oct. 2018.
- [18] Y. A. Alemu, T. T. Yetayew, and M. A. Mossie, "Transient stability enhancement of Beles to Bahir Dar transmission line using adaptive neuro-fuzzy-based unified power flow controller," *J. Electr. Syst. Inf. Technol.*, vol. 11, no. 1, p. 43, Dec. 2024.
- [19] S. Harron, V. Saxena, and N. Kumari, "Exploring the use of particle swarm optimization algorithms to enhance evolutionary computing," in *Proc. Int. Conf. Optim. Comput. Wireless Commun. (ICOCWC)*, Jan. 2024, pp. 1–6.



-
- [20] D. Wang, D. Tan, and L. Liu, “Particle swarm optimization algorithm: An overview,” *Soft Comput.*, vol. 22, no. 2, pp. 387–408, Jan. 2018.
- [21] F. Jiang, Y. Zhang, Y. Zhang, X. Liu, and C. Chen, “An adaptive particle swarm optimization algorithm based on guiding strategy and its application in reactive power optimization,” *Energies*, vol. 12, no. 9, p. 1690, May 2019, doi: 10.3390/en12091690.
- [22] M. A. Tikuneh and G. B. Worku, “Identification of system vulnerabilities in the Ethiopian electric power system,” *Global Energy Interconnection*, vol. 1, no. 3, pp. 358–365, Oct. 2018.